Scholars' Mine

Spring 2017

Generating fast and accurate compliance reports for various data rates

Srinath Penugonda

GENERATING FAST AND ACCURATE COMPLIANCE REPORTS

FOR VARIOUS DATA RATES

by

SRINATH PENUGONDA

A THESIS

Presented to the Faculty of the Graduate School of the

MISSOURI UNIVERSITY OF SCIENCE AND TECHNOLOGY

In Partial Fulfillment of the Requirements for the Degree

MASTER OF SCIENCE IN ELECTRICAL ENGINEERING

2017

Approved by

Jun Fan, Advisor
David Pommerenke
Victor Khilkevich

ABSTRACT

As the demands on the industry data rates have increased there is a need for interoperable interfaces to function flawlessly. Added to this complexity, the number of I/O data lines are also increasing making it more time consuming to design and test. This in general leads to creating of compliance standards to which interfaces must adhere. The goal of this theses is to aid the Signal Integrity Engineers with a better and fast way of rendering a full picture of the interface compliance parameters.

Three different interfaces at various data rates were chosen. They are: 25Gbps Very Short Reach (VSR) based on Optical Internetworking Forum (OIF), Mobile Industry Processer Interface (MIPI) particularly for camera based on MIPI Alliance organization upto 1.5Gbps and for a passive Universal Serial Bus (USB) Type-C cable based on USB organization particularly for generation-I with data rate of 10Gbps.

After a full understanding of each of the interfaces, a complete end-to-end reports for each of the interfaces were developed with an easy to use user interface. A standard one-to-one comparison is done with commercially available software tools for the above mentioned interfaces. The tools were developed in MATLAB and Python. Data was usually obtained by probing at interconnect, from either an oscilloscope or vector network analyzer.

ACKNOWLEDGMENTS

I would like to thank Dr.Jun Fan for giving me this opportunity and without whom this research wouldn't possible. I am thankful for him for providing the insights and guiding me through some very difficult situations. I would also like to express my sincere gratitude to Dr.Victor Khilkevich and Dr.David Pommerenke for their support and encouragement. I am also thankful to Dr.James Drewniak for his mentoring and motivation. I am great full to all the faculty of EMC Laboratory, Missouri S&T for sharing their priceless knowledge with me. I thank all my friends in the EMC Laboratory for their immense help throughout my Master's program.

Last, but not the least, I would like to thank my family for their constant support and encouragement.

TABLE OF CONTENTS

LIST OF ILLUSTRATIONS

LIST OF TABLES

LIST OF ACRONYMS

RJ	RANDOM JITTER
DJ	DETERMINISTIC JITTER
PDF	PROBABILITY DENSITY FUNCTION
CDF	CUMILATIVE DENSITY FUNCTION
UI	UNIT INTERVAL
BER	BIT ERROR RATE
EH6	EYE HEIGHT AT BER 10^{-6}
EH15	EYE HEIGHT AT BER 10^{-15}
EW6	EYE WIDTH AT BER 10^{-6}
EW15	EYE WIDTH AT BER 10^{-15}
RN0	RANDOM NOISE LEVEL-0
RN1	RANDOM NOISE LEVEL-1
ASIC	APPLICATON SPECIFIC INTEGRATED CIRCUIT
QSFP	QUAD SMALL FACTOR PLUGGABLE
VSR	VERY SHORT REACH
RMS	ROOT MEAN SQUARE
HS	HIGH SPEED
LP	LOW POWER
MIPI	MOBILE INDUSTRY PROCESSOR INTERFACE
HTML	HYPERTEXT MARKUP LANGUAGE
USB	UNIVERSAL SERIAL BUS
GND	GROUND
NEXT	NEAR END CROSS TALK
FEXT	FAR END CROSS TALK
IRL	INTEGRATED RETURN LOSS
IMR	INTEGRATED MULTI REFLECTIONS
INEXT	INTEGRATED NEAR END CROSSTALK
IFEXT	INTEGRATED FAR END CROSSTALK

1. INTRODUCTION

With increasing number of high speed interfaces within an electronic system and those connecting from outside world, there is growing need for these interfaces to be working hand in hand without any errors.

In this thesis we will look into compliance reports developed for different interfaces operating at different data rates ranging from 1Gbps to 25 Gbps. Various tools were developed from scratch using Python and MATLAB that make the work of a signal integrity engineer much easier in examining the compliance when accomplishing a complex design. With more number of interfaces, these tools come in handy too.

The following 3 sections describe the generation of compliance reports for 25Gbps Very Short Reach (VSR) based on Optical Internetworking Forum (OIF), Mobile Industry Processer Interface (MIPI) particularly for camera based on MIPI Alliance organization and for a passive Universal Serial Bus (USB) Type-C cable based on USB organization particularly for generation II.

For the 25Gbps VSR, a detailed step by step methodology is employed in determining the generation of eye characteristics to calculating the random jitter which is shown. The improvement of the eye diagram when continuous time linear equalizer (CTLE) or a feed forward equalizer (FFE) or a decision feedback equalizer (DFE) or when a combination of the above three equalizers are applied is also shown.

For the MIPI interface, calculation of rise times, fall times for high speed and low power data is shown. The increase in the eye opening after the de-embedding procedure is also shown.

For the USB Type-C, a detailed compliance report with Insertion loss fit, integrated crosstalk noise, insertion and return loss is shown. A detailed step by step methodology for measuring a USB Type-C cable to creating a compliance report is explained.

2.   RENDERING OF EYE DIAGRAM

Eye diagrams have become a norm for SI engineers in deducing the effects of channel on a data/clock signal. An eye diagram is generated by cutting the data/clock for certain period of time (usually called as unit interval (UI)) and overlaying over one another.

Though very simple, we can derive a number of parameters from the eye diagrams. Figure 2.1 shows a simple eye diagram with a good eye opening. By good eye opening, it means how much window is present for the clock to sample the data without an error in decision making. This definition of how good is the opening keeps changing from standard to standard.

There are two parameters that can be infer from eye opening – eye height and eye width. From the eye height we can deduce how much the amplitude of a signal is attenuated due to channel or simply the signal to noise ratio. With eye width we can obtain how bad the rise time of the signal has degraded when passed through the channel or simply a measure of jitter.
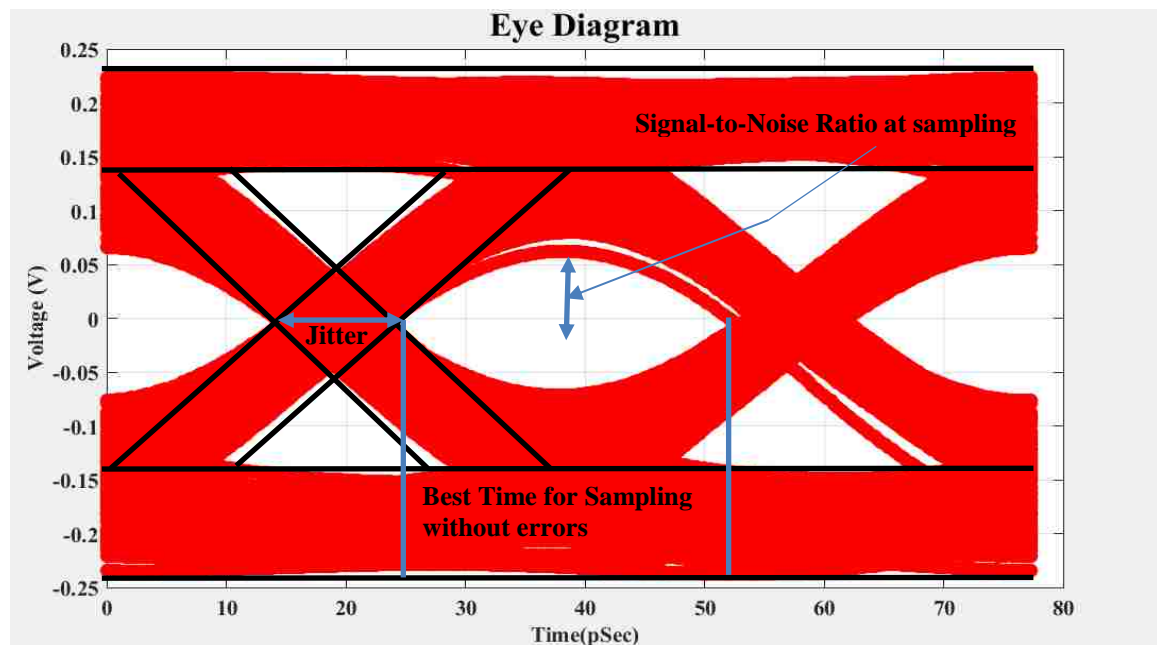
Figure 2.1 Simple Eye Diagram with Eye Opening

For calculation of eye parameters, the rendering of eye diagram is slightly modified. The axis of both time and voltage are discretized to form bins as shown in Figure.2.2 and each point in the time domain waveform is mapped to one bins. This procedure is usually referred to bin mapping. Usually, the bin size of the time axis is left equivalent to the oscilloscope settings when the signal is measured. The voltage axis is usually discretized based on the amount of signal present and system memory available.
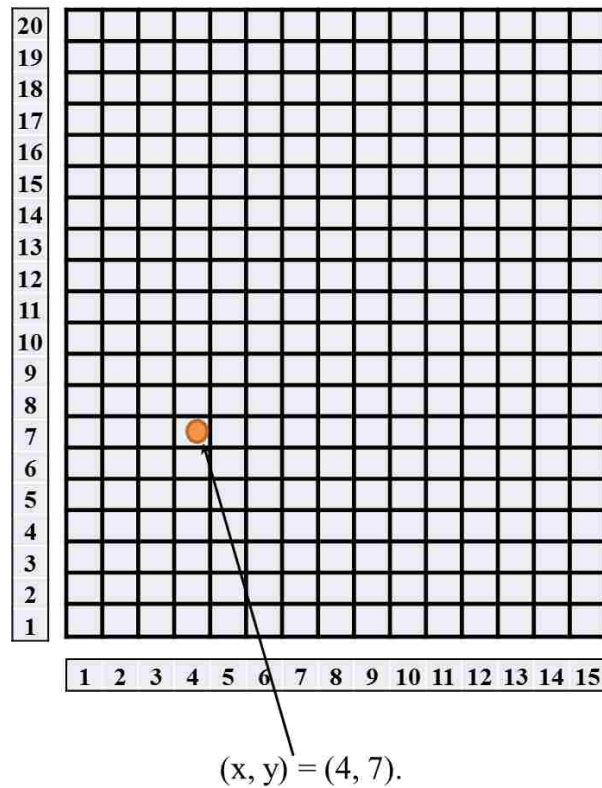
$(x, y) = (4, 7).$

Figure 2.2 Bin Mapping of Discrete Values

For example, let there be a dependent variable y =7.2 with independent variable x=4. This data point will be mapped to the (x, y) = (4, 7). By this way a record of where each bit is going can be maintained along with the count of number hits for a bin. This would later be used to find the jitter along with other eye parameters. The smaller the Δy lesser the error due to mapping. Figure 2.2 shows this example

3. PARAMETERS DEDUCED FROM EYE DIAGRAMS

3.1 CALCULATION OF RANDOM JITTER

While the calculation of eye height is pretty straight forward, the calculation of jitter is not as straight forward as eye height. This is because jitter primarily consists of random jitter (RJ) and Deterministic Jitter (DJ). There are series of steps involved in calculating random jitter as shown in Figure 3.1. PDF is Probability Density Function and CDF is Cumulative Density Function. The next few paragraphs explain each of the steps shown in Figure 3.1[1].
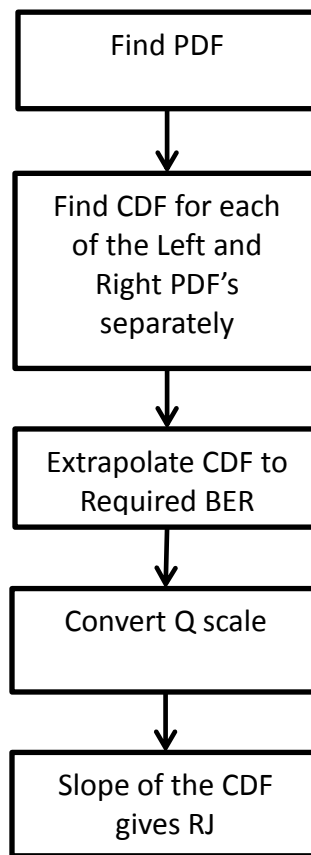
Figure 3.1 Steps to Calculate RJ from Eye Diagram

For calculating the PDF we use the bin mapped eye diagram rather than the normal way plotting eye. From the bin mapped eye we get the number of hits on each bin across the line of interest. The line of interest us usually at the zero crossing for a differential signal and average the leve-1 and level-0 for a single ended signal. Then, divide the each of this with the total number of bins along the bins. This gives us the probability of error at the zero crossing for the data or indirectly the probability density function. Figure 3.2 shows the PDF for eye diagram in Figure 2.1, both for left zero crossing and right zero crossing. Ideally, the PDF should look like a Gaussian curve. The
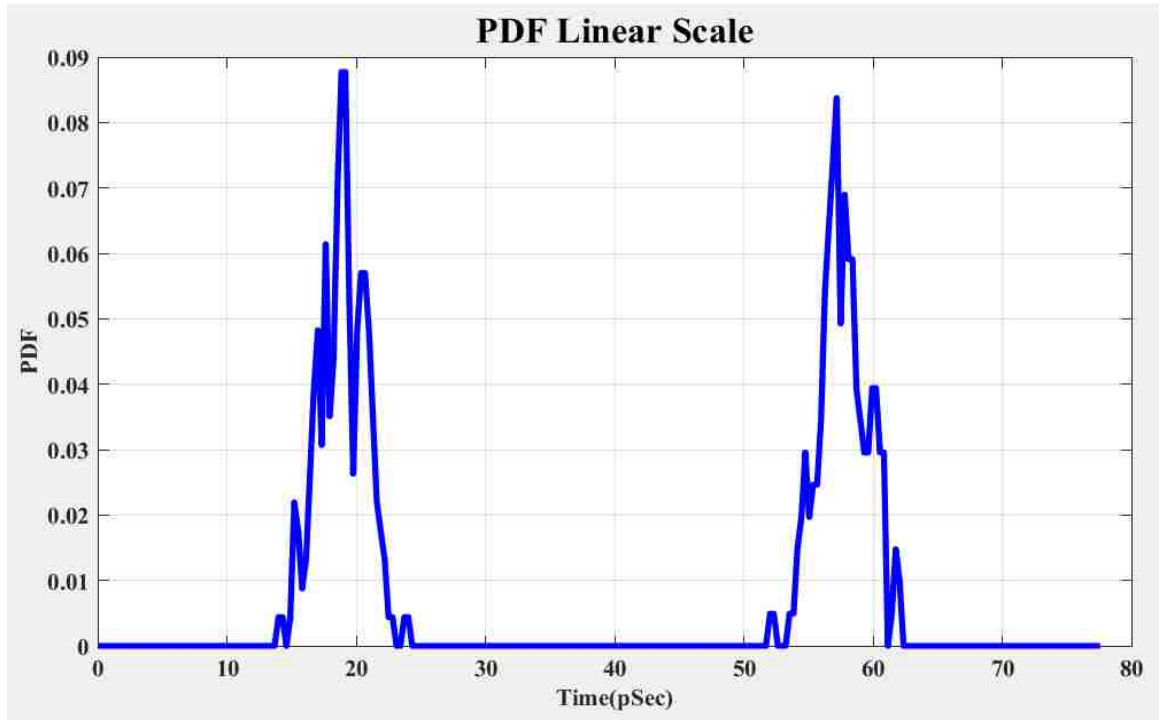
Figure 3.2 Probability Density Function for eye in Figure 2.1

curve in Figure 3.2 approaches a Gaussian function when there are infinite number of data waveforms present.

Assuming Figure 3.2 to be Gaussian functions, to obtain the CDF, integration of the curve is taken. To achieve this numerically, area under the curve is take using trapezoid method. The integration is done for left and right PDFs separately.

$$CDF(BER) = \rho_t \sum_{-\infty}^{\infty} PDF \tag{1}$$

Figure 3.3 gives an example for an ideal case. The area found out for each trapezoid is added cumulatively from right to left for obtaining CDF. The assumption made here is that Δt value is linear and very small. More explanation for calculating the bit transition ratio (ρ_t) is provided in the Section 3.2. Figure 3.4 shows the CDF of the PDF presented in Figure 3.2. As mentioned earlier, the integration is performed separately for left and right PDFs. The Figure 3.4 is often referred to as bath tub curves. The scale BER (CDF) as one of the main drawbacks that it doesn't have a linear part for finding the slope of which is the RJ part. Also, the linear part helps in extrapolation to the

$$Q(BER) = \sqrt{2}erf^{-1}[1 - \frac{1}{\rho_T} BER] \tag{2}$$

target BER. Eq .2 converts the BER (CDF) to Q (BER). Once Q-(BER) is calculated, it can be extrapolated to desired BER. Figure 3.5 is the CDF in Q-Scale for PDF in Figure 3.2.
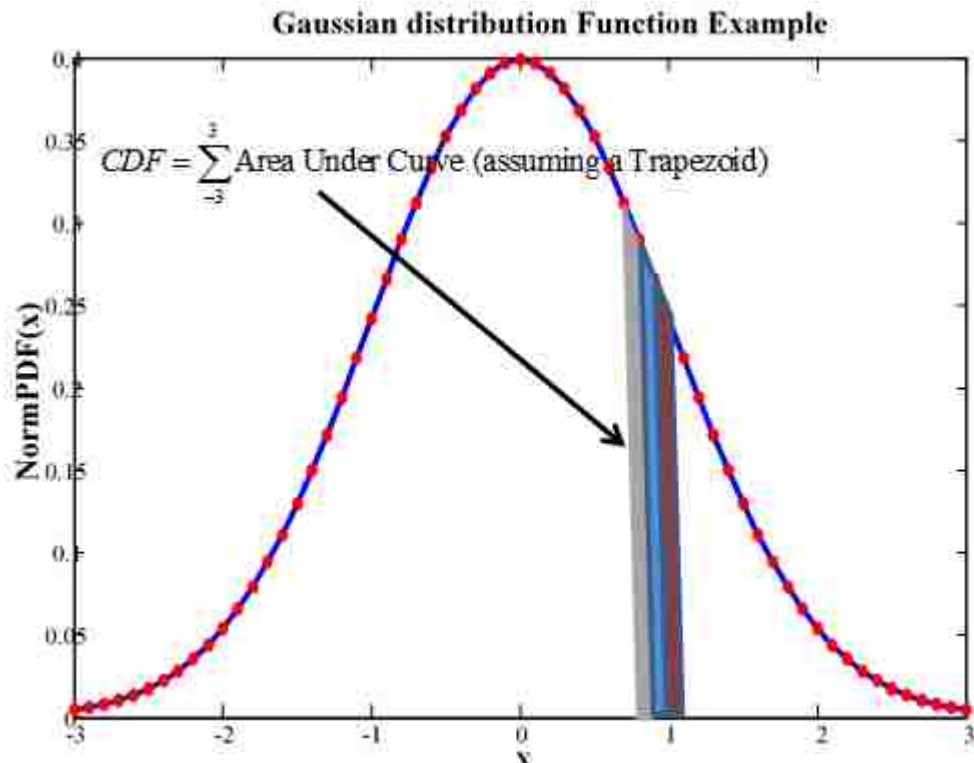
Figure 3.3 Ideal case for calculating CDF from PDF
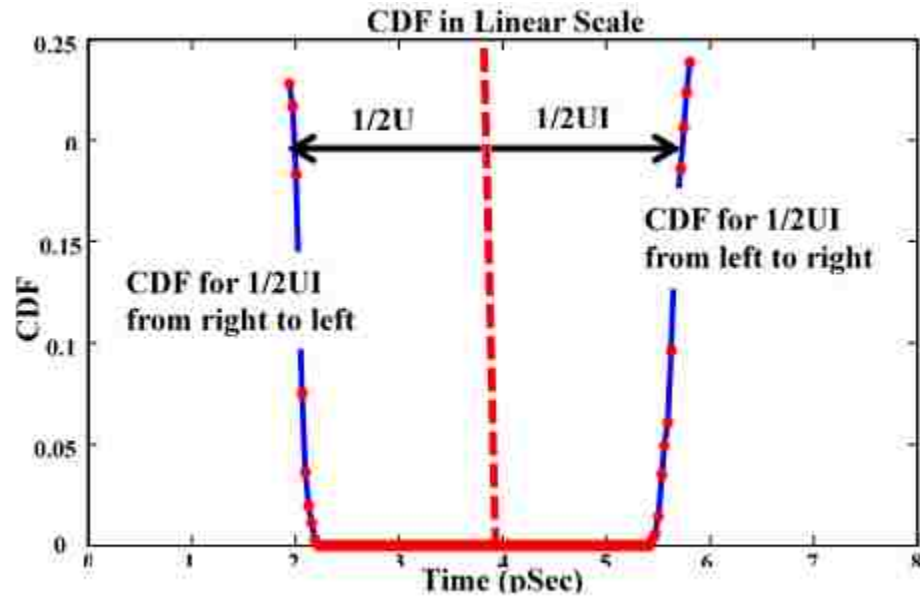
Figure 3.4 CDF of PDF present in Figure 3.2
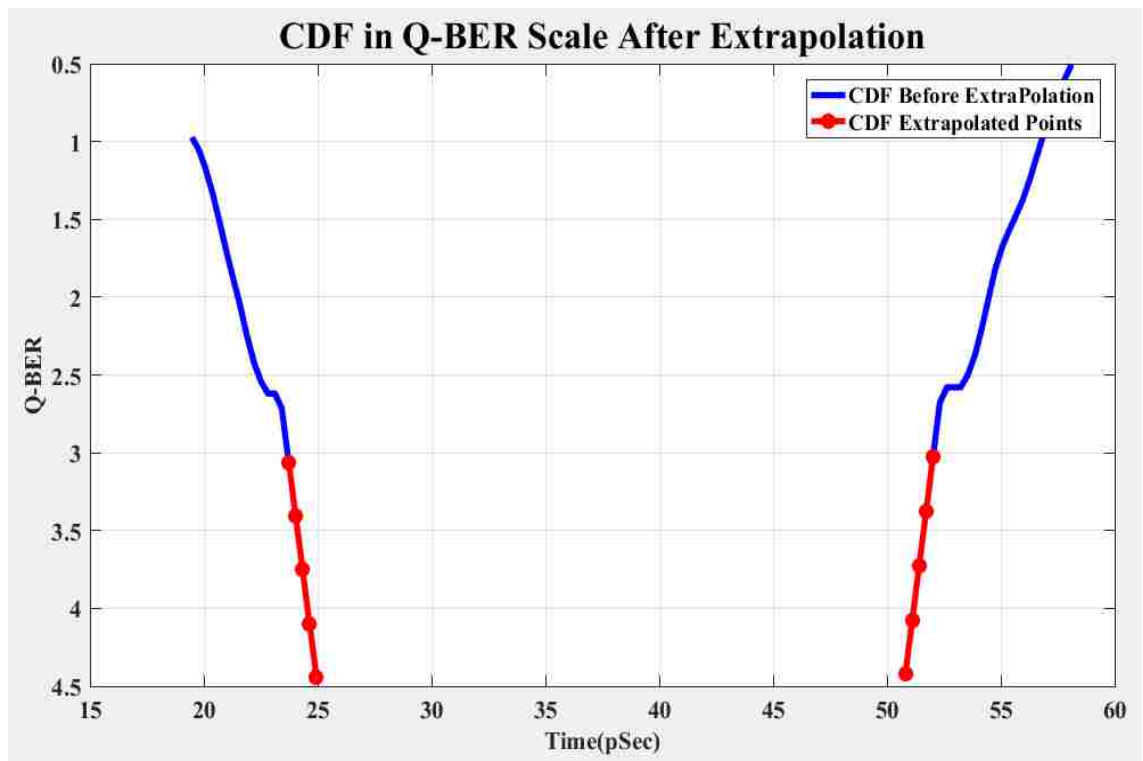
Figure 3.5 CDF in Q-Scale after Extrapolating to Q=4.5

3.2 BIT TRANSITION RATIO

The bit transition ratio (ρ_t) is the total number of bits to that of total number of transitions from level 0 to level 1 and level-1 to level-0. This can be easily found out if we can identify the zero crossings of edges. If there is no exact location at the zero-crossing, a point can be interpolated using the adjacent points at 0V. Total number of bits is the ratio of difference between clock edges and the UI. Theoretically, for a pseudo random bit sequence (PRBS) this value is equal to 0.5. Practically, due to jitter this value is close to 0.5. Hence, it is important to calculate ρ_t . Figure 3.6 gives the next step for finding the CDF.

$$\text{bitTransition ratio} = \left[\frac{\text{Total. no of Bits}}{\text{ClockEdges}} \right] \tag{3}$$

$$\text{Total No. of bits} = \text{round} \left[\frac{\text{Difference between Clock Edges}}{\text{Unit Interval}} \right] \tag{4}$$

3.3 INVERSE OF SLOPE OF THE CDF

The inverse of slope of the linear part of the CDF gives the RJ part from the total jitter. Slope has to be calculated separately for left and right CDF. In most cases, there is requirement for a linear extrapolation to higher Q values of interest. The DJ part can also be obtained using a dual-dirac modelling of total jitter. The same process is applied to find the vertical bathtub curves and horizontal bath tub curves.

CDF in Q-BER Scale After Extrapolation
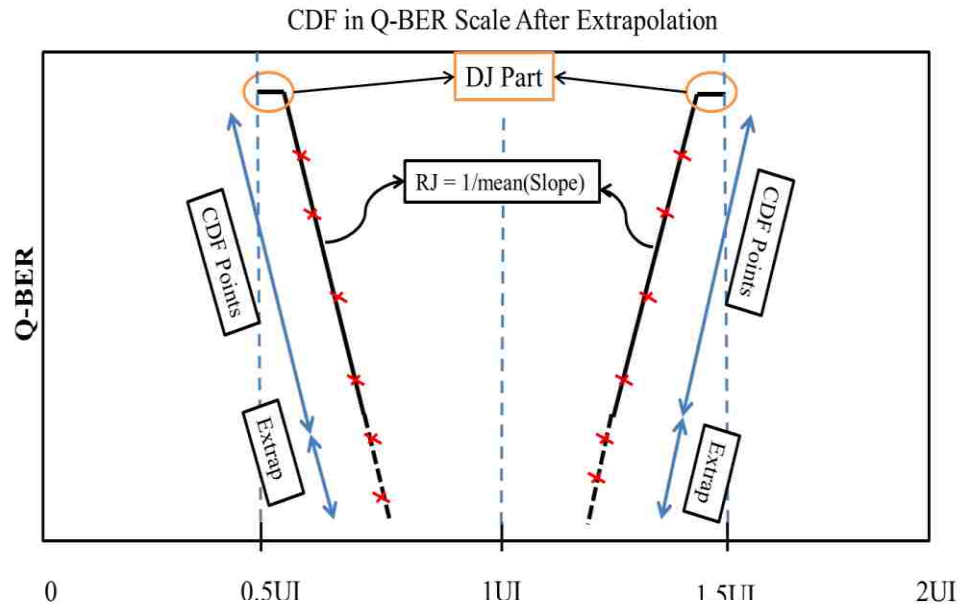
Figure 3.6 CDF in Q-BER Scale Identification Points

4. EQUALIZATION

4.1 OVERVIEW

An ideal interconnect channel passes signals from transmitter to destination without distortion. Practically, a signal undergoes both amplitude and phase distortion. The amplitude distortion is because of the unequal attenuation of different frequency components of the signal. Phase distortion is because of the frequency dependence of the phase components of the signal. As the frequency of operation increases, for a given material, the eye opening keeps diminishing. In other words, the high frequency components of the signal take more time to charge up the interconnect and transition to its maximum value is greater than the switching rate of the transmitter. This is the intersymbol interference (ISI) [AA]. In short, the difference between the high and low frequency losses should be negated to remove the ISI effects. This is achieved using equalization. For example, Figure 4.1 is the eye diagram after the channel and before the equalization for the data in Figure 3.1. One of the desired characteristics of an equalizer
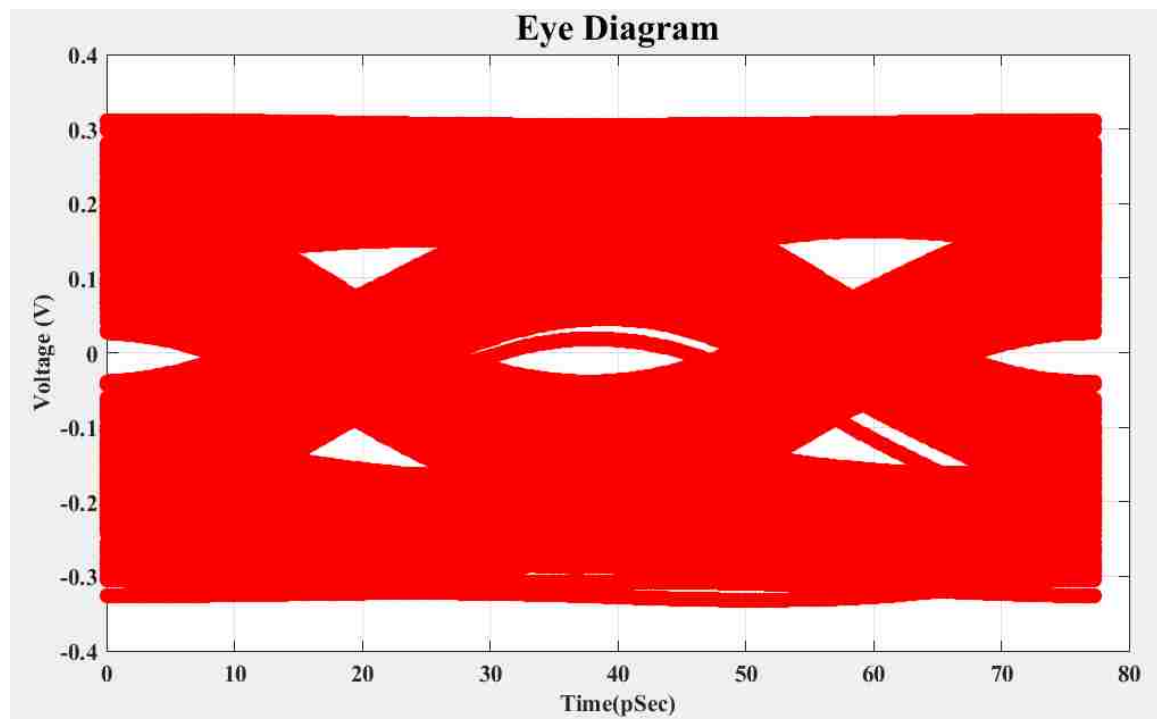
Figure 4.1 Eye Diagram before Equalization for Eye in Figure 3.1

is to amplify the high frequency and attenuate the low frequency. There are different types of equalization both are linear and non-linear. Continuous time linear equalizers are usually required to be implemented in most of the standards.

4.2 CONTINOUS TIME LINEAR EQUALIZER

The transfer function of the CTLE is shown in Eq.4. Table-4.1 gives the equalized coefficients for the rate 28GBd. Figure 4.2 shows the implementation of the CTLE transfer function for Eq 4 in MATLAB. The Figure 4.2 clear indicates the peaking at near the Nyquist frequency. This peaking value approximates the difference between

$$H(s) = \frac{(G)(P1)(P2)}{Z1} \frac{(S+Z1)}{(S+P1)(S+P2)}$$

$$S = j2\pi f$$

(5)

the low frequency gain and the high frequency gain at Nyquist in dB. This transfer function is recommended in standards [3]
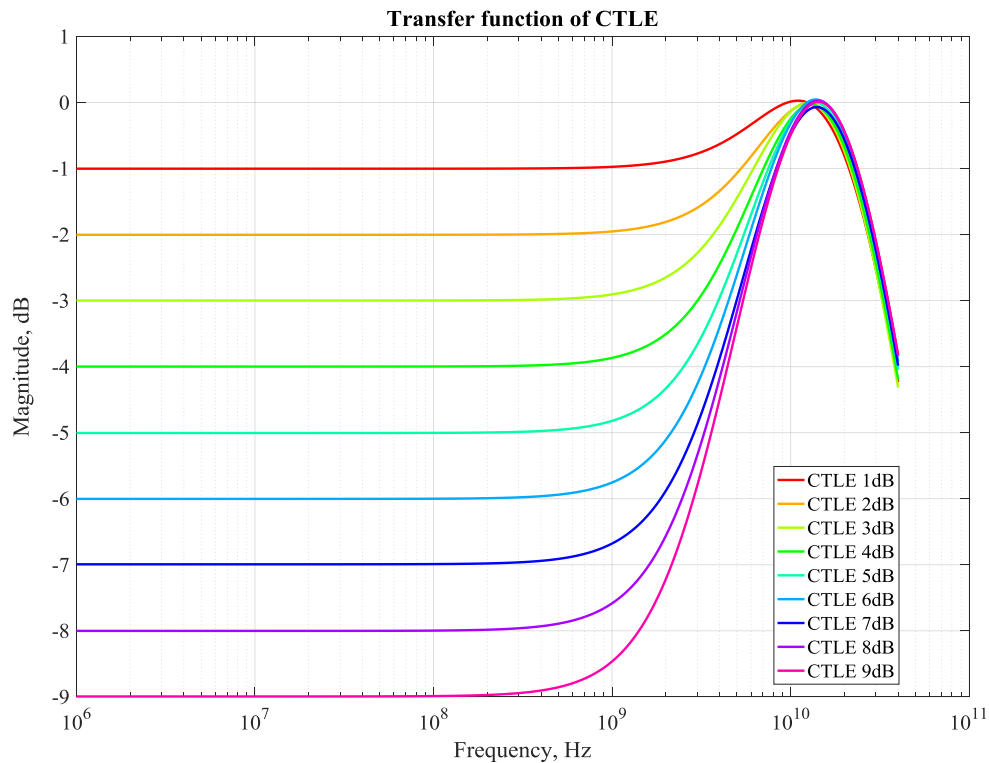
Figure 4.2 Receiver CTLE Transfer Function for Gains 1dB to 9dB

With definition of CTLE in place and the process of calculating CDF from eye diagrams, the standards for the VSR can be implemented. Section 5 describes the standards and the tool implementation in MATLAB.

Table 4.1 Coefficient values for Eq 4.2 till 28GBd

Peaking(dB)	G	$P1/2\pi$ (GHz)	$P2/2\pi$ (GHz)	$Z1/2\pi$ (GHz)
1	0.891	18.6	14.1	8.31
2	0.794	18.6	14.1	7.1
3	0.708	15.6	14.1	5.68
4	0.631	15.6	14.1	4.98
5	0.562	15.6	14.1	4.35
6	0.501	15.6	14.1	3.82
7	0.447	15.6	14.1	3.43
8	0.398	15.6	14.1	3
9	0.355	15.6	14.1	2.67

5. FEATURES INCLUDED IN THE TOOL

5.1 REQUIREMENTS BY OIF CEI COMPLIANCE STANDARDS

All the compliance standards in Section 5.1.1 to 5.1.3 are based on [2]. A differential signal obtained from the oscilloscope is used for the calculations elaborated below. Usually a PRBS9 signal is used according to the standard.

5.1 1 Eye Width. The eye width is to be calculated at 10-15. The eye width is calculated as the difference in the time between CDFL (CDF left) and CDFR (CDF Right) at the BER 10-6 and then estimated at 10-15 using the Eq 5. RJL and RJR are the RJ left and RJ right respectively. The eye width should be minimum 0.46*UI for the interface to pass the compliance.

$$EW15 = \left(EW6 - 3.19\left(RJL + RJR\right)\right) \qquad (6)$$

5.1.2 Eye Height. The eye height also has to be calculated at 10^{-15}. The eye height is calculated as the difference between the CDF1 (CDF level-1) and CDF0 (CDF level-0) at the BER 10^{-6} and then estimated at 10^{-15} using the Eq 6. RN1 and RN0 are the level-1 and level-0 random noise respectively. Random noises are similar to RJ but are related to amplitudes instead of the times. The eye height should be minimum of 95mV to pass the compliance.

$$EH15 = \left(EH6 - 3.19\left(RN0 + RN1\right)\right) \qquad (7)$$

5.1.3 Random Jitter. The differential signal is used to construct CDFs at the zero crossing and calculate the inverse of the mean of the slope of the linear part for RJ. For obtaining the RJ (RMS), divide the RJ with Q value. The methodology for the deduction of RJ is explained in Section 3.

5.2 MEASUREMENT SETUP

Following in the Figure 5.1 is the measurement setup recommended by the standards. The measurement is performed at the TP1a point. The time domain signal data is then saved as a comma separated file (CSV) on the scope which is given as an input to the 28G VSR Post Processing Tool.

TP1a

| ASIC (PRBS9) | → | QSFP Cable | → | Host Compliance Board | → | Scope |
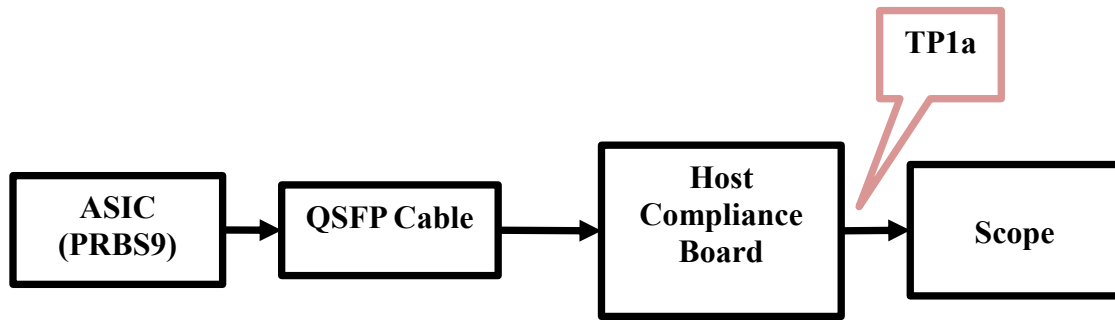
Figure 5.1 Measurement Setup for 28G VSR

6. 28G VSR POST PROCESSING TOOL USING MATLAB

The tool is capable of show casing all the features explained in Section 2-4 and render a full picture of the results as explained in Section 5.1.1-5.1.3. It is also possible to perform FIR and DFE equalization though the results are not elaborated here.Figure 6.1 shows the time domain input signal. Figure 6.2 shows the eye opening after CTLE.
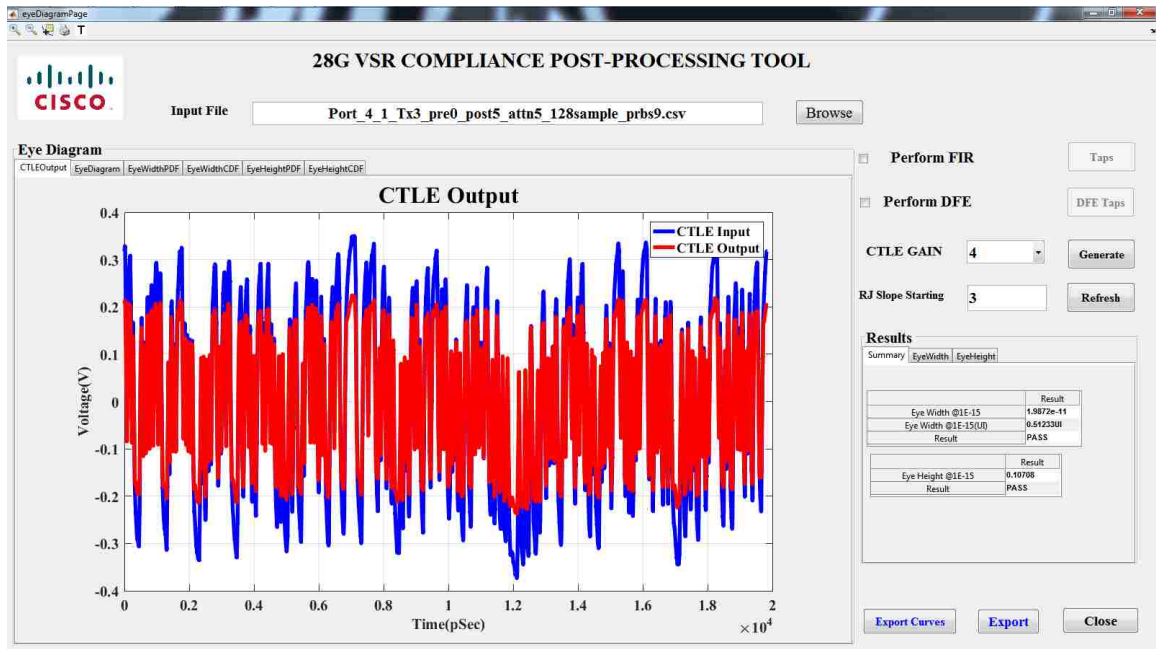
Figure 6.1 CTLE Output from the Post-Processing Tool
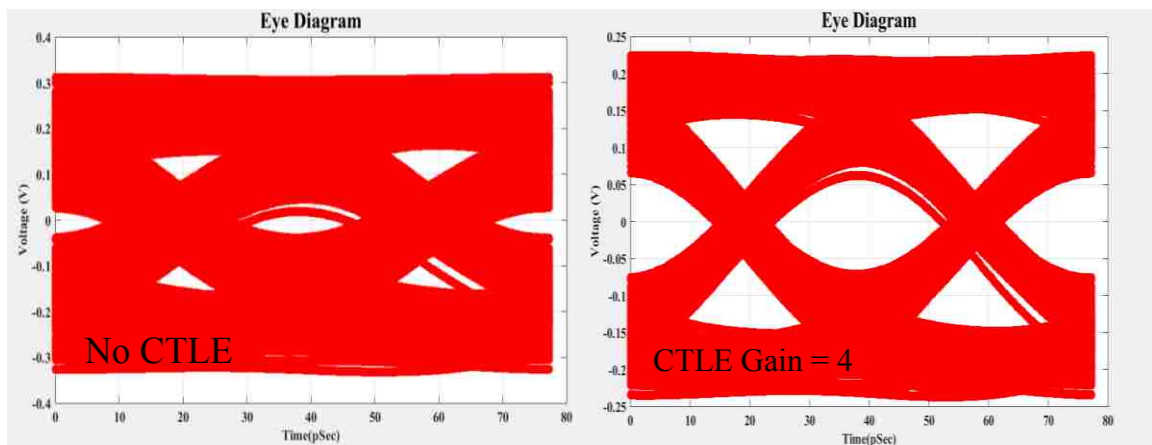
Figure 6.2 Eye Diagram before and after CTLE

6.1 ZERO CROSSING PDF AND CDF

The following Figure 6.3 represents the PDF of the Figure 6.2 and Figure 6.4 the corresponding CDF.
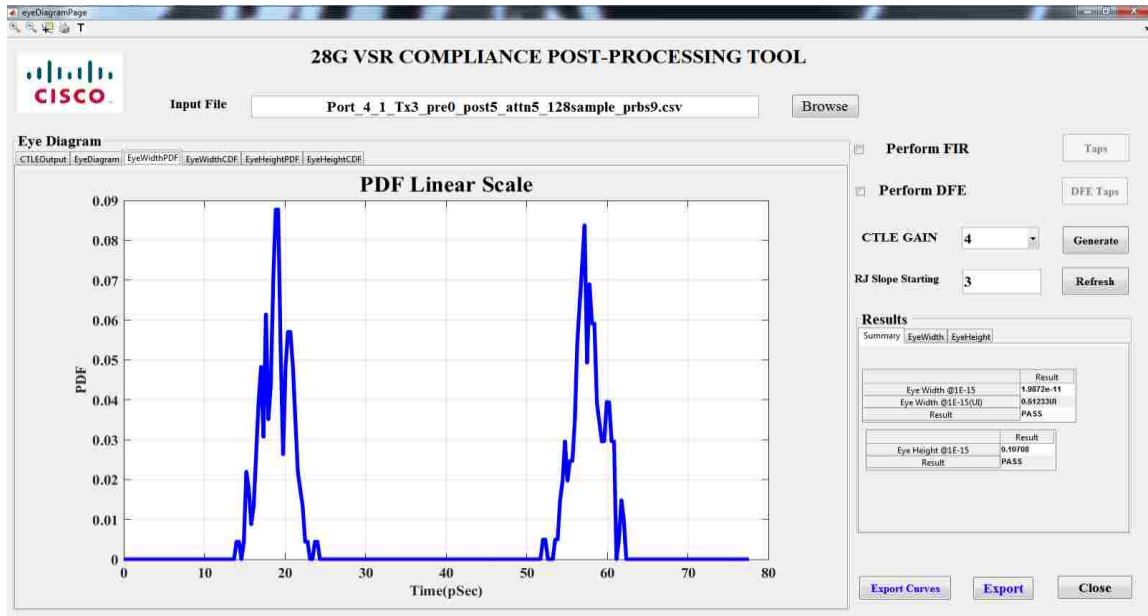
Figure 6.3 Zero Crossing PDF for the Eye Diagram in Figure 6.2 with CTLE =4dB
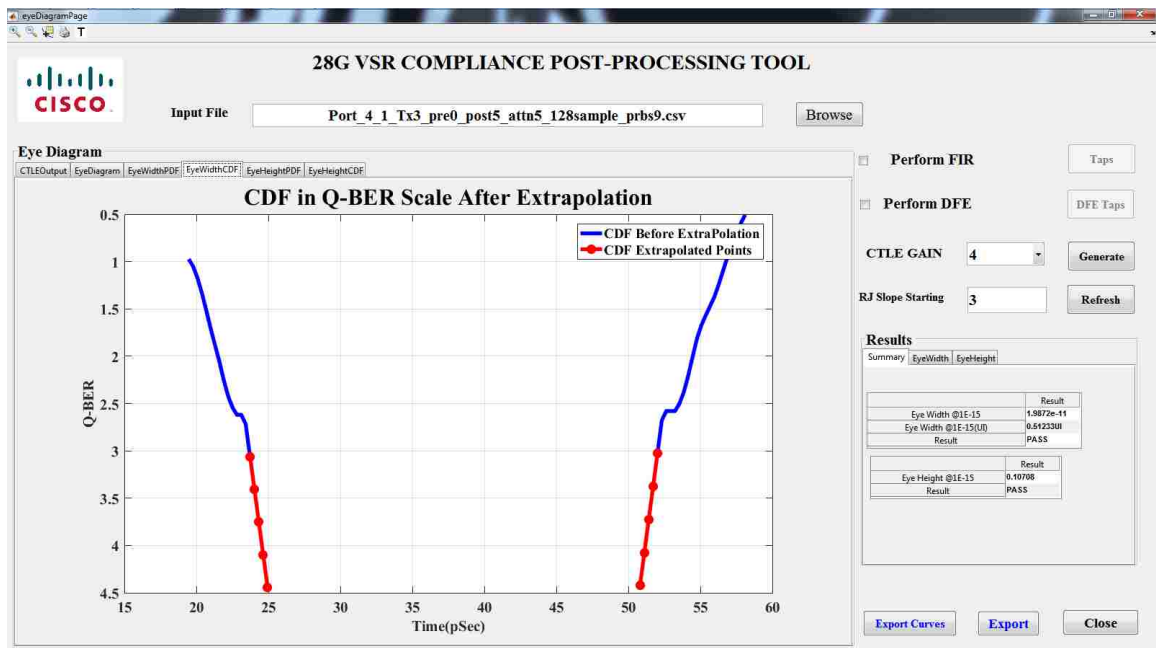
Figure 6.4 Extrapolated CDF for Zero crossing in Q-BER Scale for PDF in Figure 6.3

6.2 LEVEL-0 AND LEVEL-1 PDF AND CDF

The below Figure 6.5 discusses the PDF of the vertical 0 and 1 level crossing for eye diagram in Figure 6.2 and Figure 6.6 its corresponding CDF.
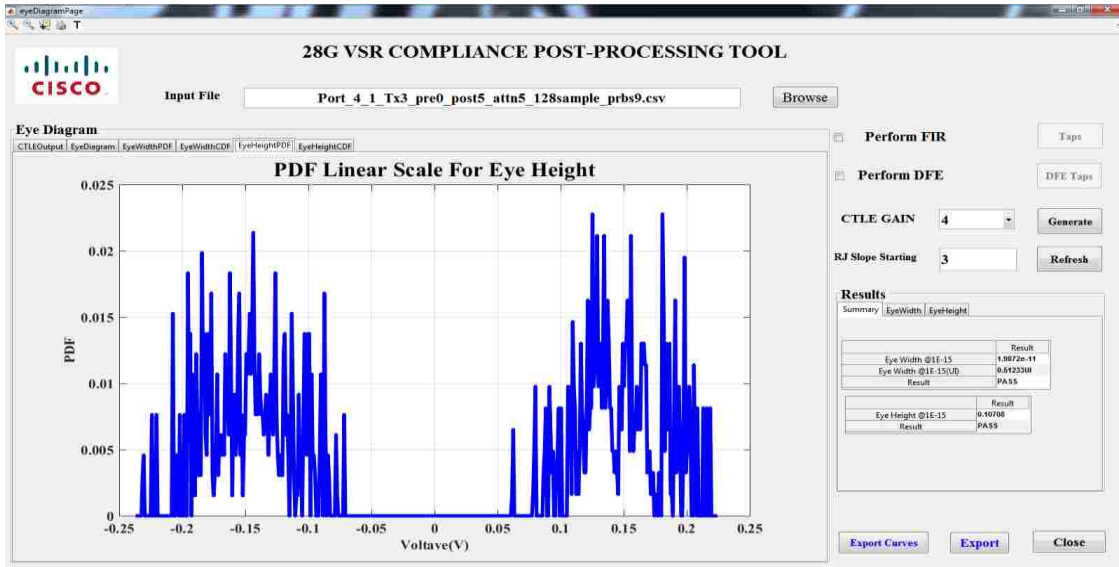
Figure 6.5 Vertical PDF for the Eye Diagram in Figure 6.2 with CTLE =4dB
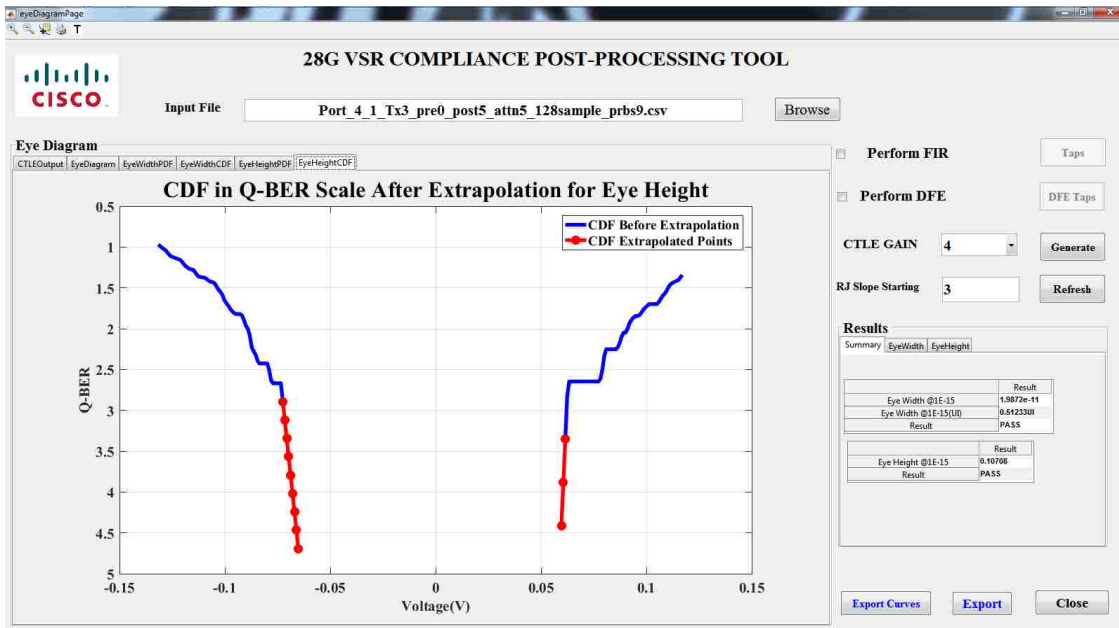
Figure 6.6 Extrapolated CDF for Level-1 and 0 in Q-BER Scale for PDF in Figure 6.5

6.3 RESULTS FOR EYE WIDTH AND EYE HEIGHT

Below Table 6.1 and Table 6.2 are the results for one set of time domain data shown in Figure 6.1.

Table 6.1 Results for Eye Width

CTLE GAIN	4
BER LEVEL	1e-06
ESTIMATION LEVEL	1e-15
Eye Height @1E-6	0.12571 V
RJL	0.0041072 V
RJR	0.0017331 V
Eye Height @1E-15	0.10708 V
Result	PASS

Table 6.2 Results for Eye Height

CTLE GAIN	4
BER LEVEL	1e-06
ESTIMATION LEVEL	1e-15
Eye Width @1E-6	2.6163e-11 Sec
RJL	1.1008-13 Sec
RJR	8.7127e-13 Sec
Eye Width @1E-15	1.9872e-11 Sec
Eye Width @1E-15(UI)	0.51233UI
Result	PASS

7. UNDERSTANDING MIPI D-PHY WAVEFORM

7.1 WAVEFORM INTRODUCTION

There are 2 states in the waveform during a normal operation –low swing high speed differential transmitting (HS) mode and high swing low power (LP) transmitting mode. These two modes differ significantly in their characteristics as shown in Figure 7.1. A detailed explanation for each of the modes and their separation methodology is explained in the subsequent Sections.

After the separation of the HS and LP, an eye diagram is rendered for the HS data, clock as explained in Section 2. A different type of eye diagram called the data to clock eye diagram is also rendered. All the possible eye parameters are also calculated except for the RJ part. Instead of the RJ, the MIPI post processing tool helps to calculate peak-to-peak jitter. Rise time and fall time of the HS and LP are also calculated along with many other parameters.

Most of the information about HS and LP data is already explained in [3]
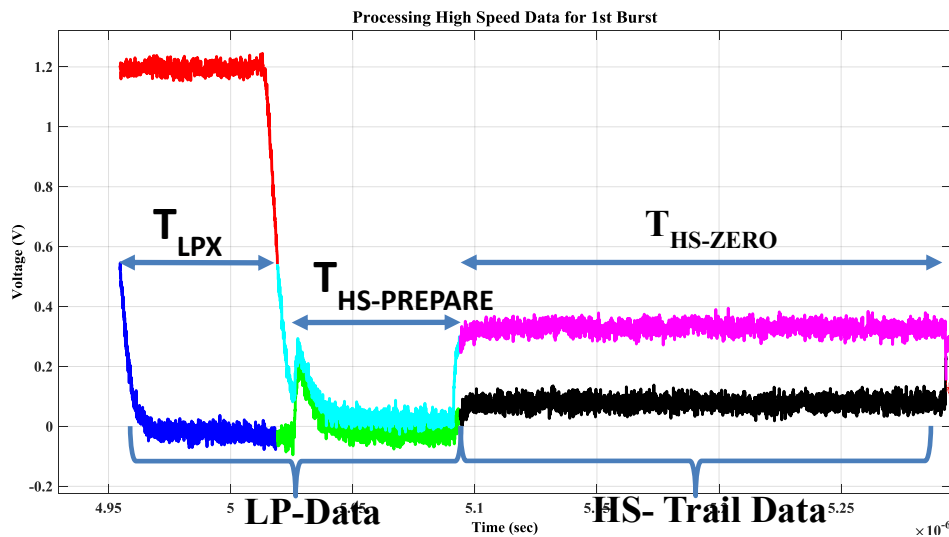
Figure 7.1 Identifying different Pattern for Separating HS and LP

7.2 HIGH SPEED (HS) AND LOW POWER (LP) DATA

The HS is operated in a differential mode. Hence, there are two possible HS lane states, differential-1 and differential-0. The bit rate range for the HS is between 80-1500Mbps and voltage swing for the differential voltage is 200mV. Figure 7.2 shows the SOT detection.

The data is transferred during the HS state only. During the idle state, the transmitter stays in the LP state. For receiver synchronization, the HS is aided with start and stop states. Also, certain data pattern is followed during the start of data transmission (SOT) and end of transmission (EOT). The same data pattern detection is followed to separate the HS from the LP data.

Steps involved for SOT:

1. Drive Stop State (LP-11)
2. Drive HS-Request State (LP-01) for T_{LPX}
3. Drive Bridge State (LP-00) for $T_{HS\text{-}PREPARE}$
4. Drive HS-0 for a time $THS_{\text{-}ZERO}$
5. Insert the HS Sync Sequence '00011101'.

Steps involved in EOT
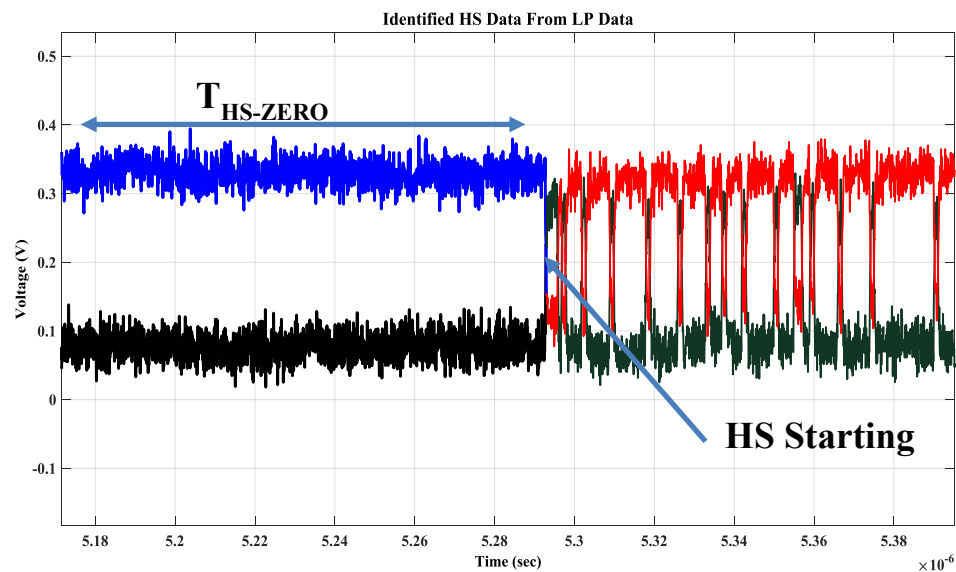
Figure 7.2 Identified HS Data

1. Toggle the differential state immediately after last payload data bit and keep the state for a time $T_{HS\text{-}TRAIL}$.
2. Disable the HS-TX and enable the LP-TX, drive the stop state LP-11 for a time $T_{HS\text{-}EXIT}$.

The LP data is single ended with two lanes driving independently. All the LP state periods should be at least T_{LPX}. The voltage level of the LP signal is from 10mV to 1.2V. The clock is also separated in the same way as the data. Figure 7.3 shows the LP detection when signal leaves from HS to LP.
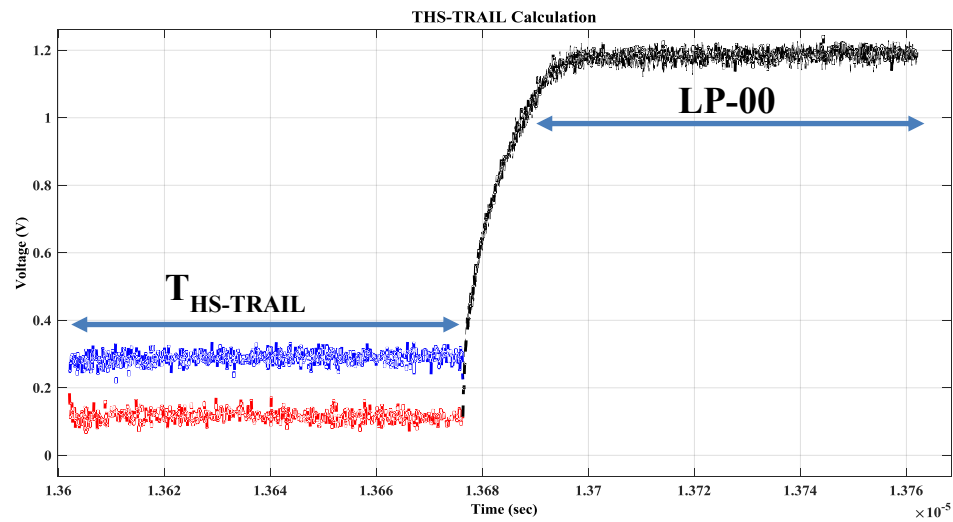
Figure 7.3 THS-TRAIL Calculation

8. MIPI POST-PROCESSING TOOL OVERVIEW

8.1 FLOW DIAGRAM

Figure 8.1 shows different pages available in the tool and their respective tabs.
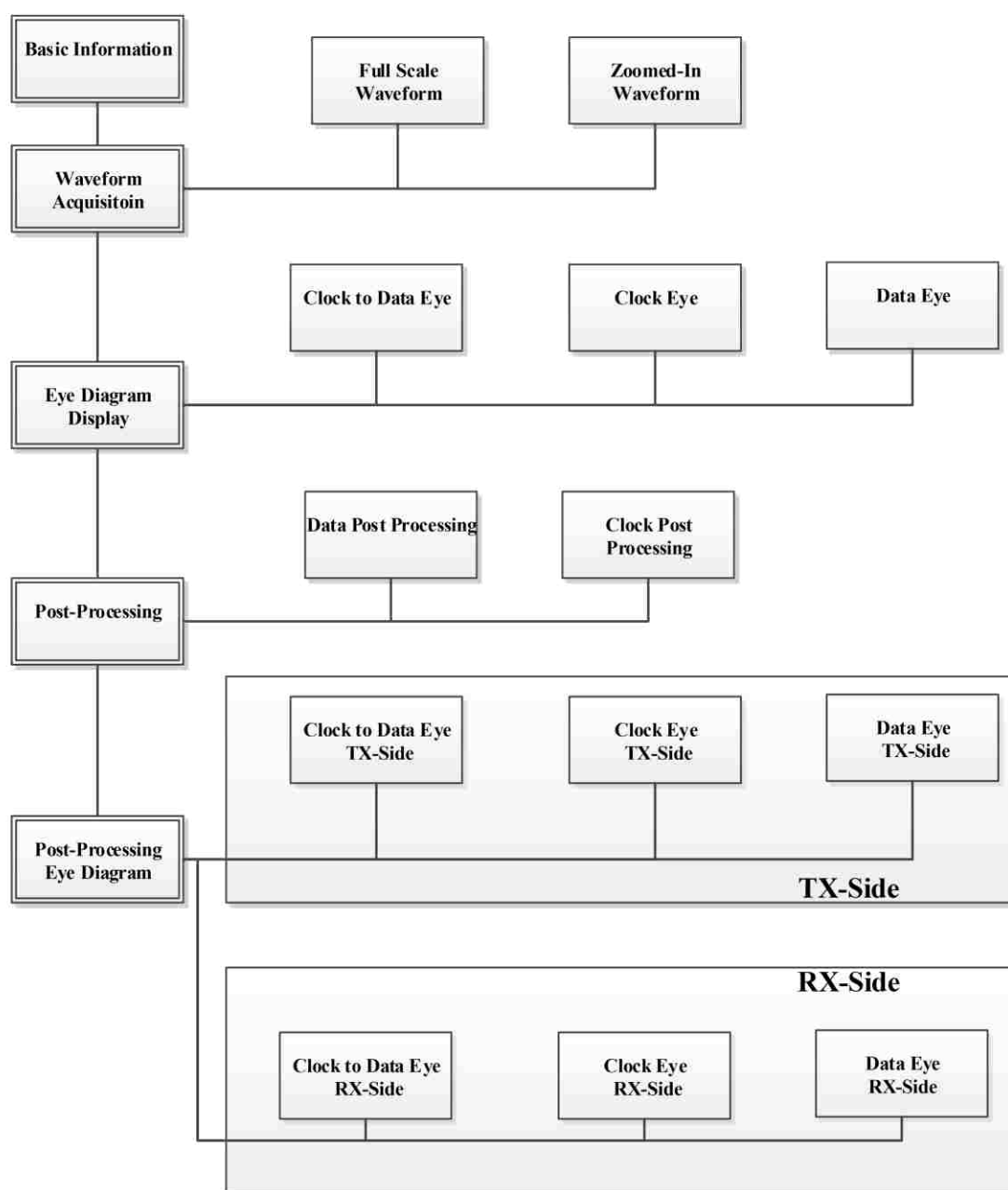
Figure 8.1 Tool Flow Diagram

8.2 WAVEFORM ACQUISITION PAGE

The waveform is captured automatically from the oscilloscope. Auto waveform capturing allows the tool to capture the data multiple times until a good waveform is detected. Figure 8.2 shows one of the two captured signals. Since, the HS waveform is important for rendering an eye diagram, it needs to be captured with better voltage resolution. An automatic scaling is done to set the best voltage resolution. The tool has feature to perform the automatic scaling and capture. If the captured signal can't be separated into LP and HS, the tool re-captures the signal automatically. A convenient way of selecting and searching of the instruments connected to the tool is also available. There is no user intervention needed while capturing the waveform. A detailed logging is also available at every step.

Figure 8.2 Waveform Capture Page

8.3 EYE DIAGRAM DISPLAY

The Eye diagram display page displays different eye diagrams,

1. Data-Clock,
2. Clock,
3. Data eye diagrams.

A quick summary of calculated P-P Jitter, eye height, rise and fall time, and UI are shown. For a detailed report, there is a HTML report created when the "Generate Report" feature is accessed. The report generated is for the data measured after the common-mode choke, between camera sensor and the common mode choke. A feature to import an eye mask file or create is also available. A detailed report of different parameters required for the MIPI standards can be viewed by clicking on "Generate Report". Figure 8.3 shows the Data-to-Clock Eye diagram

Figure 8.3 Eye Diagram Page

8.4 COMPLIANCE REPORT

There are 3 different sections in the report each for

1. High Speed Data
2. High Speed Clock
3. Low Power Data and timing

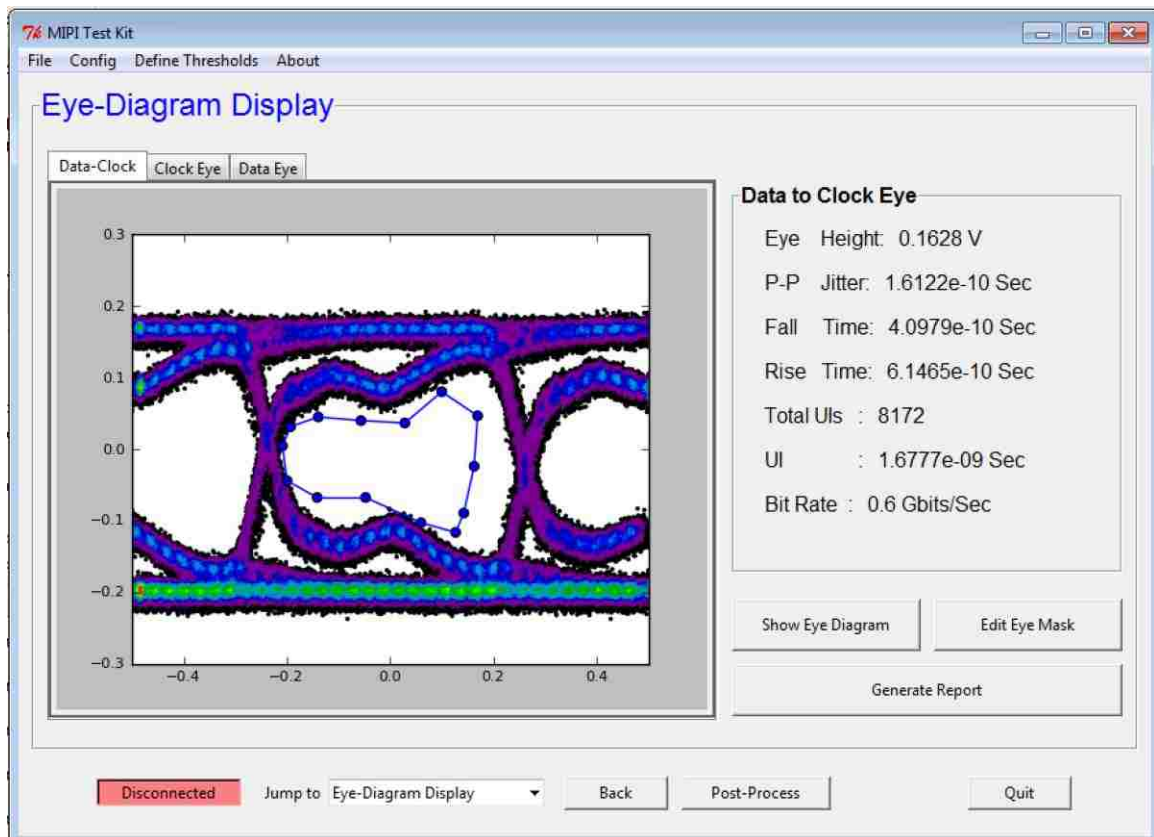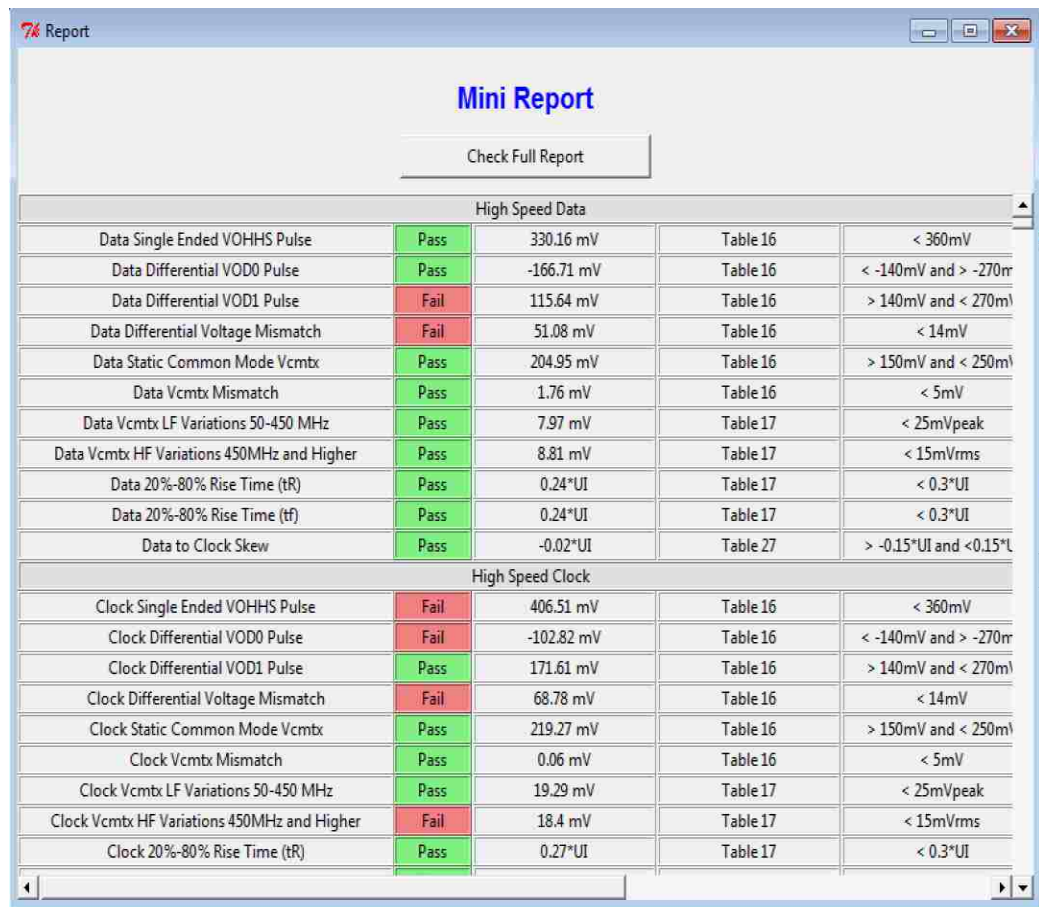A mini report containing the compliance parameters calculated is presented as shown below in Figure 8.4. A HTML report is also generated which shows plots of all the parameters suggested by the MIPI standards document. A detailed comparison between a commercially available tool and MIPI Post-Processing Tools explained here is shown below in Table 8.1.

7k Report				
Mini Report				
Check Full Report				
High Speed Data				
Data Single Ended VOHHS Pulse	Pass	330.16 mV	Table 16	< 360mV
Data Differential VOD0 Pulse	Pass	-166.71 mV	Table 16	< -140mV and > -270m
Data Differential VOD1 Pulse	Fail	115.64 mV	Table 16	> 140mV and < 270mV
Data Differential Voltage Mismatch	Fail	51.08 mV	Table 16	< 14mV
Data Static Common Mode Vcmtx	Pass	204.95 mV	Table 16	> 150mV and < 250mV
Data Vcmtx Mismatch	Pass	1.76 mV	Table 16	< 5mV
Data Vcmtx LF Variations 50-450 MHz	Pass	7.97 mV	Table 17	< 25mVpeak
Data Vcmtx HF Variations 450MHz and Higher	Pass	8.81 mV	Table 17	< 15mVrms
Data 20%-80% Rise Time (tR)	Pass	0.24*UI	Table 17	< 0.3*UI
Data 20%-80% Rise Time (tf)	Pass	0.24*UI	Table 17	< 0.3*UI
Data to Clock Skew	Pass	-0.02*UI	Table 27	> -0.15*UI and <0.15*U
High Speed Clock				
Clock Single Ended VOHHS Pulse	Fail	406.51 mV	Table 16	< 360mV
Clock Differential VOD0 Pulse	Fail	-102.82 mV	Table 16	< -140mV and > -270m
Clock Differential VOD1 Pulse	Pass	171.61 mV	Table 16	> 140mV and < 270mV
Clock Differential Voltage Mismatch	Fail	68.78 mV	Table 16	< 14mV
Clock Static Common Mode Vcmtx	Pass	219.27 mV	Table 16	> 150mV and < 250mV
Clock Vcmtx Mismatch	Pass	0.06 mV	Table 16	< 5mV
Clock Vcmtx LF Variations 50-450 MHz	Pass	19.29 mV	Table 17	< 25mVpeak
Clock Vcmtx HF Variations 450MHz and Higher	Fail	18.4 mV	Table 17	< 15mVrms
Clock 20%-80% Rise Time (tR)	Pass	0.27*UI	Table 17	< 0.3*UI

Figure 8.4 Mini-Report Containing Parameters Suggested by Standards

8.5 POST PROCESSING

The tool also provides a detailed post processing page, where users can input the load R, C and get the de-embedded time domain waveform and the time domain waveforms at the load side. Suitable S-Parameters are to be provided to get the eye diagrams. Figure 8.5 shows the input page for post processing. The loading condition is flexible and different R, C values can be given and the eye parameters at the load side and the transmitter side can be calculated.

Table 8.1 Comparison of various Parameters between Keysight and EMC Lab Tool

Parameter Name	Keysight Result	EMC Lab Result
1.3.7 HS Data TX Static Common Mode Voltage(Vcmtx)	178.89 mV	180.56 mV
1.3.8 HS Data TX Vcmtx Mismatch	1.36 mV	3.51 mV
1.3.10 HS Data TX Common-Level Variations Above 450MHz (VCMTX(HF))	5.94 mV	2.05 mV
1.3.9 HS Data TX Common-Level Variations Between 50-450MHz (VCMTX(LF))	12.20 mV	11 mV
1.3.4 HS Data TX Differential Voltage(VOD)	190.20 mV	207 mV
1.3.5 HS Data TX Differential Voltage Mismatch	19.55 mV	25 mV
1.3.6 HS Data TX Single Ended Output High Voltage(VOHHS)	316.74 mV	308.11 mV
1.3.11 HS Data TX 20%-80% Rise Time (tR)	516 ps	540 ps
1.3.12 HS Data TX 20%-80% Fall Time (tF)	518 ps	540 ps
1.5.4 Data-to-Clock Skew (TSKEW(TX))	77 mUIinst	60 mUI
1.4.7 HS Clock TX Static Common Mode Voltage(Vcmtx)	184.30 mV	185.07 mV
1.4.8 HS Clock TX Vcmtx Mismatch	600 µV	0.05 mV
1.4.10 HS Clock TX Common-Level Variations Above 450MHz (VCMTX(HF))	6.58 mV	1.21 mV
1.4.9 HS Clock TX Common-Level Variations Between 50-450MHz (VCMTX(LF))	8.83 mV	0.0 mV
1.4.4 HS Clock TX Differential Voltage(VOD)	181.90 mV	181.19 mV
1.4.5 HS Clock TX Differential Voltage Mismatch	24.42 mV	12.12 mV
1.4.6 HS Clock TX Single Ended Output High Voltage(VOHHS)	324.08 mV	327.16 mV
1.4.11 HS Clock TX 20%-80% Rise Time (tR)	467 ps	456ps
1.4.12 HS Clock TX 20%-80% Fall Time (tF)	468 ps	456ps

Figure 8.6 shows the post-processed eye diagram from the MIPI Post-Processing Tool and the Keysight tool.
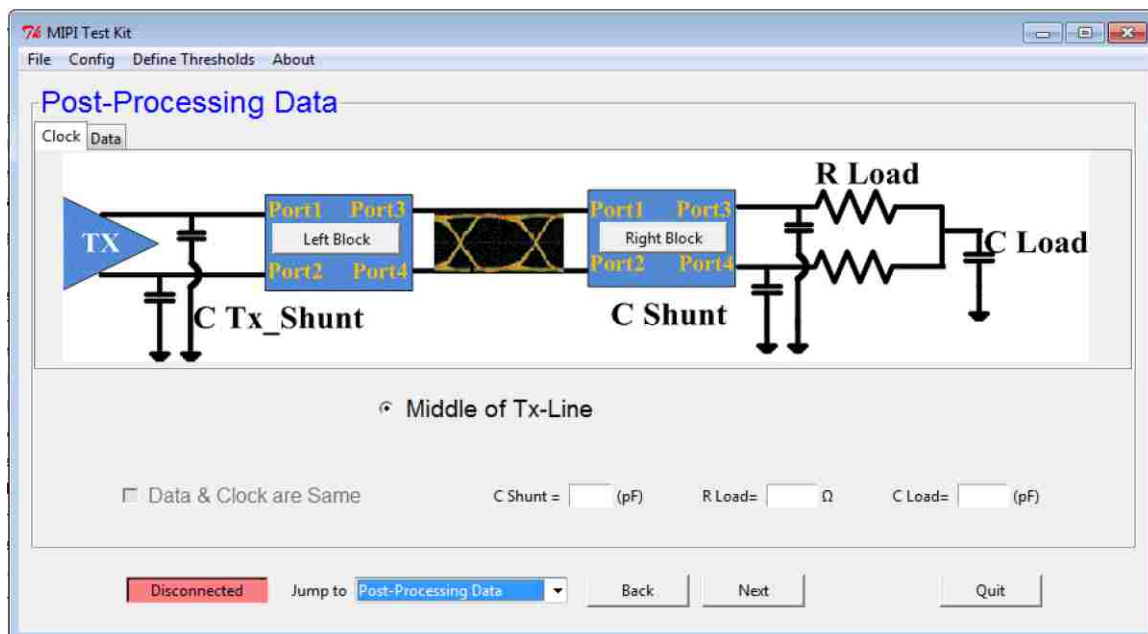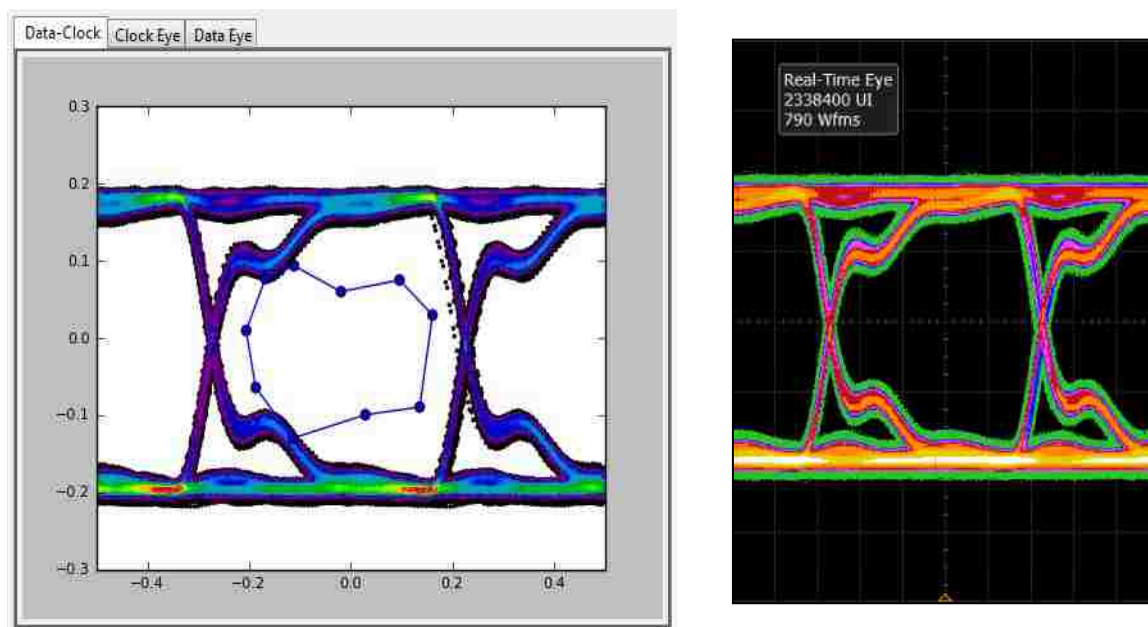

Figure 8.5 Post-Processing Page

Figure 8.6 Post-Processing Comparison between MIPI Tool and Keysight Tool

9. INTRODUCTION TO USB TYPE-C

9.1 CABLE RECEPTACLE AND DATA RATES

The data rate of operation for a generation 2 USB SuperSpeed Gen 2 is up to 10Gbps. The future generation is expected to have a possible data rate of 20 Gbps[4]. The following is the receptacle interface front view in Figure 9.1. Not all the signals shown in the Figure 9.1 are required in all platforms or devices

GND	TX1+	TX1-	Vbus	CC1	D+	D-	SBU1	VBUS	RX2-	RX2+	GND
GND	RX1+	RX1-	Vbus	SBU2	D-	D+	CC2	Vbus	TX2-	TX2+	GND

Figure 9.1 USB Type-C Receptacle Interface (Front View)

The D+/D- signals are relevant to the USB 2.0 version. So, the USB Type-C delivers both the USB 2.0 and USB Type-C data rates. The multiple locations would facilitate being able to functionally map the USB signals independent of plug orientation in the receptacle. The Figure 9.2 is a sample measurement setup
There are 4 groups of wires:

1. USB D+/D-
2. USB SuperSpeed signal Pairs
3. Side Band Wires
4. Power and GND WiresVconn (optional)

9.2 CALCULATION OF ELECTRICAL CHARACTERSTICS

There are 4 different compliance parameters being calculated. They are:

9.2.1 Insertion Loss at Nyquist. Measures the loss at Nyquist frequency, the measured cable assembly differential insertion loss is fitted with smooth function as in Figure 9.3. Any standard fitting algorithm can be used to fit the insertion loss and find the ILfitatNq.

Figure 9.2 USB Type-C Passive Cable Measurement

The ILFitatNq shall meet the following requirements for different data rates.

– ≥ −4 dB at 2.5 GHz for 5Gbps,

– ≥ −6 dB at 5 GHz, for 10Gbps,

– ≥ −11 dB at 10 GHz for

In this application we are concerned only till 10Gbps or Gen 1. The following is an example representation of Insertion loss fit and ILFitatNq calculation.
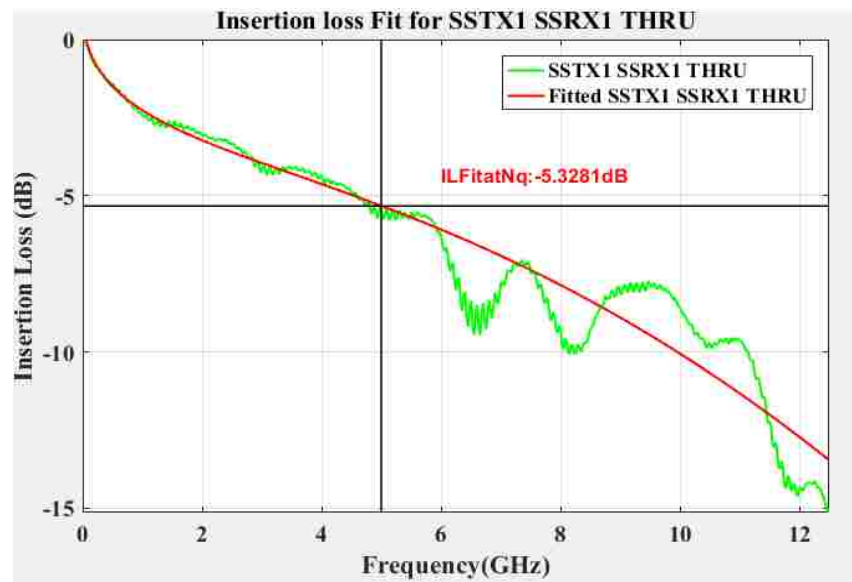

Figure 9.3 Representation of Insertion Loss Fit and ILFitatNq

In this application we are concerned only till 10Gbps or Gen 1. The following is an example representation of Insertion loss fit and ILFitatNq calculation.

9.2.2 Integrated Multi-Reflections (IMR). Measures the ripple of the insertion loss caused by multiple reflections inside the cable assembly. The insertion loss deviation's integration for the pulse response with the input voltage pulse of T_r rise time and T_b fall time is defined as the IMR as shown in Figure 9.4.

The insertion loss deviation is defined

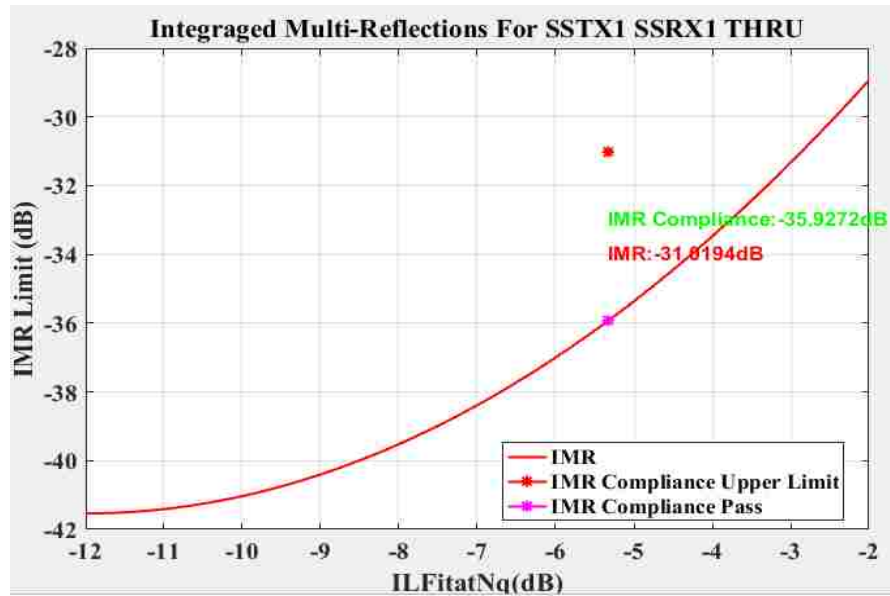$$ILD(f) = IL(f) - ILfit(f) \tag{8}$$

Figure 9.4 Representation of IMR versus ILFitatNq

Then, IMR is given and IMR Limits are given by

$$IMR = dB \left(\sqrt{ \frac{\int_0^{f_{max}} |ILD(f)|^2 |Vin(f)|^2 \, df}{\int_0^{f_{max}} |Vin(f)|^2 \, df} } \right) \; and, \; |Vin(f)| = \left| \frac{\sin(\pi f T_r)}{\pi f T_r} \cdot \frac{\sin(\pi f T_b)}{\pi f T_b} \right|$$

$$IMR \leq 0.126 * ILfitatNq^2 + 3.024 * ILfitatNq - 23.392 \tag{9}$$

9.2.3 Integrated Crosstalk between Superspeeds (INEXT, IFEXT). The integrated crosstalk between all USB SS pairs is calculated using the following formulae Where NEXT(f), FEXT(f) and C2D(f) are measured near end and far end cross talk between USB SS pairs and common-mode-to-differential conversion respectively. NEXTd(f) and FEXTd(f) are far and near-end crosstalk from D+/D- pair to SS pairs Vdd(f) is the input pulse spectrum evaluated using the equation with Tb=2.08ns The coupling between the other combinations of USB SS pairs is comparatively lower. The largest values of INEXT and IFEXT shall meet the following requirements

$$
\text{INEXT} = \text{dB}\left[\sqrt{\frac{\int_0^{f_{max}} |Vin(f)|^2 \left(|NEXT(f)|^2 + 0.125^2 |C2D(f)|^2\right)df + |Vdd(f)|^2 |NEXTd(f)|^2 df}{\int_0^{f_{max}} |Vin(f)|^2}}\right] \tag{10}
$$

- INEXT, IFEXT <-40dB

9.2.4 Integrated Return Loss (IRL). The integrated return loss (IRL) manages the reflection between the cable assembly and the rest of the systems. It is defined as The Figure 9.5 shows the example of IRL versus ILFitatNq

$$
IRL \le 0.046 * ILfitatNq^2 + 1.812 * ILfitatNq - 10.784 \tag{11}
$$

$$
IRL = dB\left(\sqrt{\frac{\int_0^{f_{max}} |Vin(f)|^2 |SDD21(f)|^2 \left(|SDD11(f)|^2 + |SDD22(f)|^2\right)df}{\int_0^{f_{max}} |Vin(f)|^2 df}}\right) \tag{12}
$$

9.3 USB TYPE-C TO TYPE-C COMPLIANCE TOOL

The Figure 9.6 shows the landing page. The landing page lest the user select if the measurement is already performed or, start with a new cable measurement. A procedure to input the files measured separately has also been incorporated.
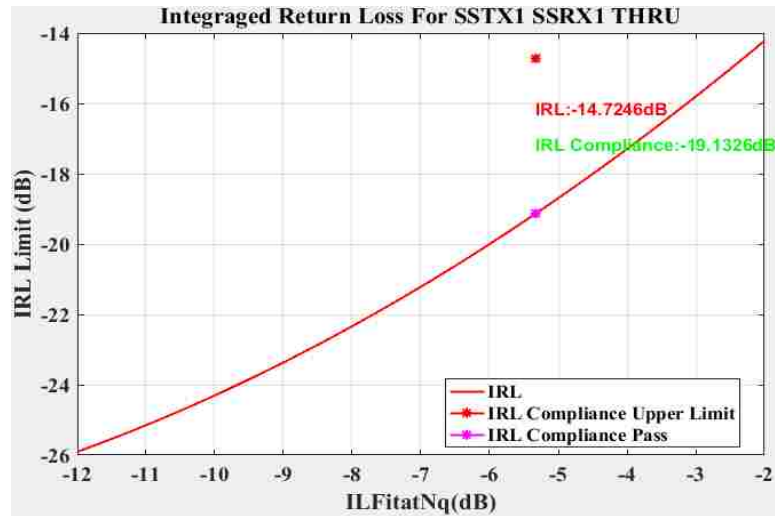
Figure 9.5 Representation of IRL at ILFitatNq

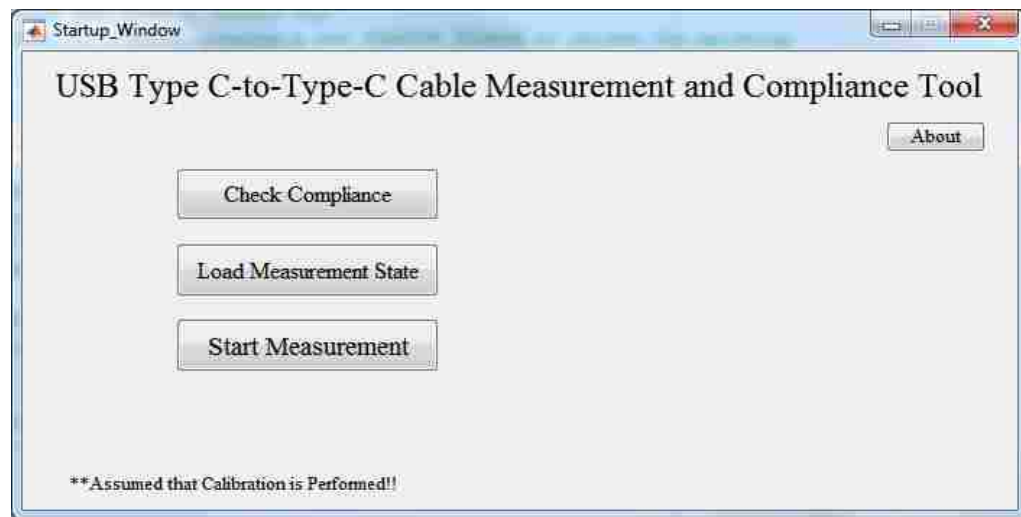Figure 9.7 shows the window for loading the S-parameters already measured separately.

Figure 9.6 Landing Page

The Figure 9.8 shows the measurement window. It is just like any other assistive measurement window, can automatically connect to the VNA and fetch S-Parameters. This window also helps to guide a user to what ports needs to be connected to the compliance board.

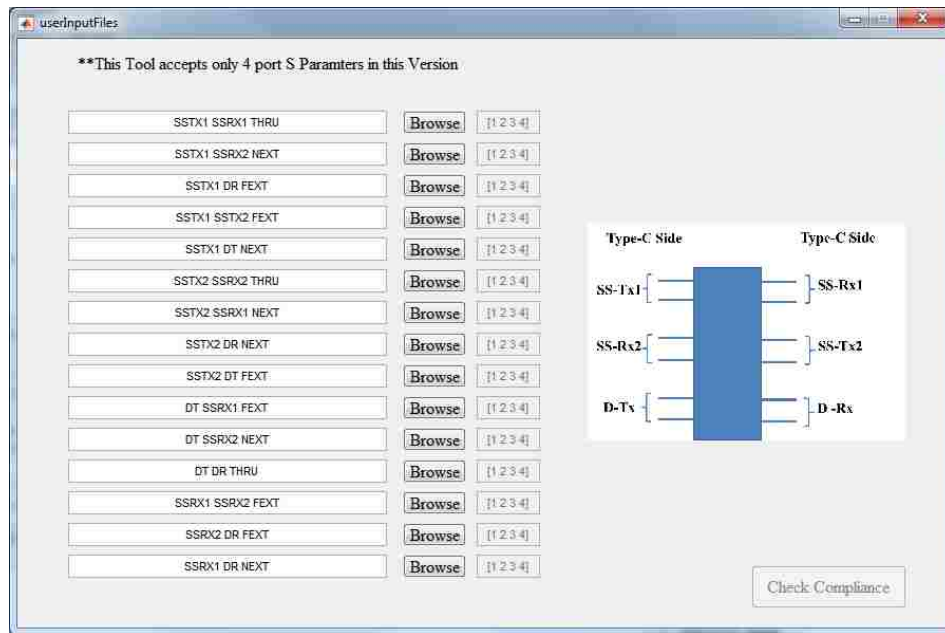The Figure 9.8 shows the compliance window where the results are displayed.

Figure 9.7 Window for Input files measured separately

The window helps the user in selecting which compliance result to be calculated and a detailed plot is also shown. A detailed report can also be exported into an MS Excel document.

9.4 RESULTS COMPARISON

This is a high level comparison between USB org tool and EMC Lab tool. There is a slight difference between ILfit, IMR and IRL. This may arise due to difference in the fitting algorithm. The standards don't mention to use a specific fitting algorithm, rather asks to implement a generalized algorithm. A detailed analysis is being carried out on why the INEXT and IFEXT delta values are more. Table 9.1 shows the results obtained using EMC Lab tool as compared to USB Org Tool.

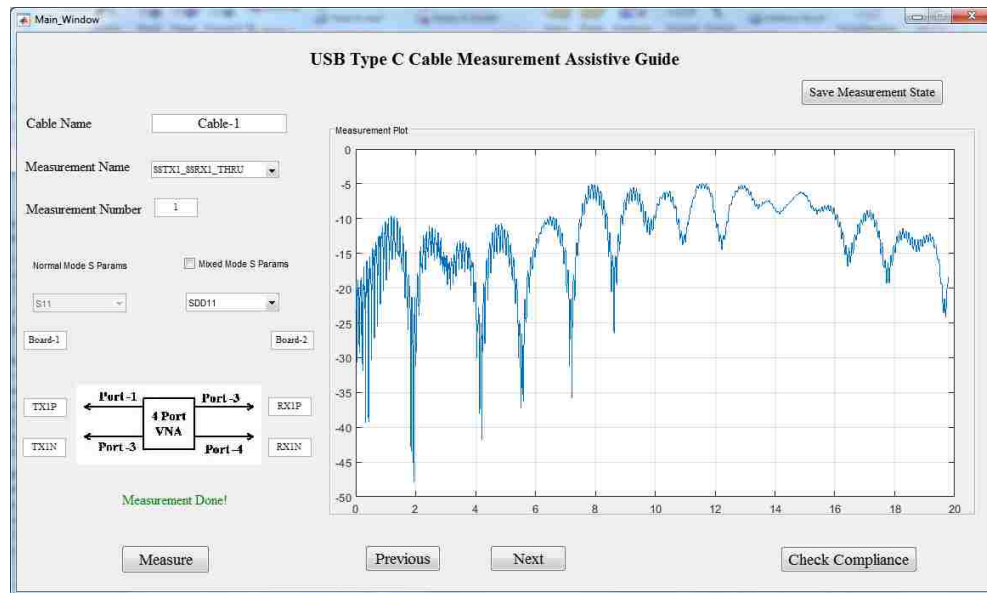The Figure 9.9 shows the example measurement window.

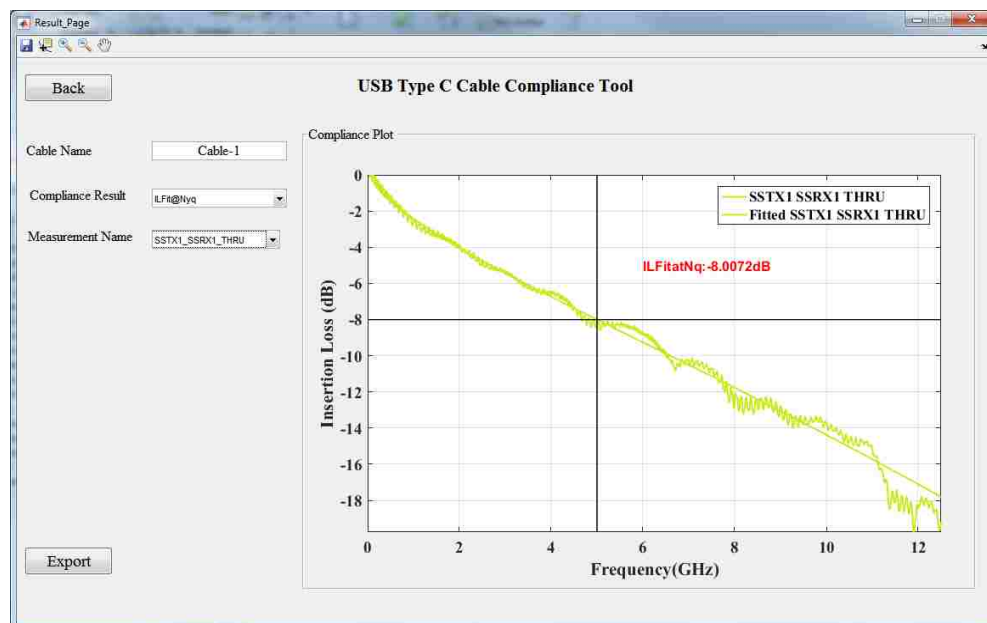Figure 9.8 Measurement and User Guiding Window

Figure 9.9 USB Type-C Compliance Results Window

Table 9.1 Results Comparison EMC Lab Tool against USB Org tool

	USB Org Tool (dB)	EMC Lab Tool(dB)	Delta(dB)
ILfit@2.5GHz, dB	-5.1	-4.76	0.34
ILfit@5.0GHz, dB	-8.2	-8.007	0.193
ILfit@10.0GHz, dB	-14.7	-14.3	0.4
IMR, dB	-32.7	-34.2	-1.5
IRL, dB	-16	-17.2	-1.2
INEXT, dB	-44.6	-57.2	-12.6
IFEXT, dB	-44.5	-55	-10.5
SCD12/SCD21, dB	-20.9	-20.2	0.7
D+/D- IL@50MHz, dB	-0.62	-0.7673	-0.1473
D+/D- IL@100MHz, dB	-1.08	-0.9311	0.1489
D+/D- IL@200MHz, dB	-1.56	-1.3059	0.2541
D+/D- IL@400MHz, dB	-2.15	-1.8479	0.3021

.

10. CONCLUSION

The compliance reports for various data rates as below are discussed. For each of the cases a detailed comparison of the reports against commercial tools has been provided. The speed at which the compliance reports are generated are also discussed. A detailed algorithm for efficiently separating the Jitter components was given.

1. 25G+ VSR for 25Gbps
2. MIPI for 1.5 Gbps
3. USB Type C-to-Type C

REFERENCES

[1]   Keysight White Paper 5989-9337EN, "Jitter Analysis: The dual-Dirac Model, RJ/DJ, and Q-Scale.

[2]   Optical Internetworking Forum Common Electrical I/O, "IA Title: Common Electrical I/O (CEI) - Electrical and Jitter Interoperability agreements for 6G+ bps, 11G+ bps and 25G+ bps I/O".

[3]   MIPI Alliance, "MIPI D-PHY Specification v1.1"

[4]   USB 3.0 Promoter Group, "USB Type-C Specification Release v1.1".

[5]   ON Semiconductor AND9075/D "Understanding Data Eye Diagram Methodology for Analyzing High Speed Digital Signals".

VITA

Srinath Penugonda received his Masters degree from department of Electrical Engineering at Missouri University of Science and Technology in May 2017. He joined in EMC laboratory in the same university as a Graduate Research Assistant in May 2014 and since then has been involved in various research projects with Dr.Jun Fan. His main research interests include signal integrity and electromagnetics.